

Two-dimensional dusty plasma crystals and liquids

Z. Donkó^{1,2}, P. Hartmann^{1,2}, G. J. Kalman²

¹ Research Institute for Solid State Physics and Optics of the Hungarian Academy of Sciences, Budapest, Hungary

² Physics Department, Boston College, Chestnut Hill, MA, USA

E-mail: donko@mail.kfki.hu

Abstract. Strongly coupled plasmas – in which the average potential energy per particle dominates over the average kinetic energy – appear in a wide variety of physical systems. Among these systems, dust plasma crystals and liquids realized in low-pressure gas discharges by dispersing mesoscopic grains into the plasma have attracted a lot of attention during the past years. We describe the experimental realization of the quasi-two-dimensional dust system, summarize the basics of the computer simulation and theoretical approaches capable of their description in the liquid and solid phases. We discuss the properties of the dynamical density and current correlation spectra, generated by molecular dynamics simulations, and address the issues associated with the existence of different phases and transport coefficients (e.g. superdiffusive behavior) in the low-dimensional systems under study.

1. Introduction

In the majority of types of plasmas the kinetic energy of the particles is significantly higher than the potential energy arising from the interaction of the charged particles. Such plasmas are conventionally termed as “ideal” ones. In contrast with these, in “non-ideal plasmas” the interaction energy already plays a role in the physics of the systems. The (less frequent) cases when the potential energy dominates over the kinetic energy are termed as “strongly coupled plasmas”. As examples of strongly coupled plasmas those appearing in some astrophysical objects (white dwarf interiors, neutron star crusts, supernova cores, and giant planetary interiors), semiconductor devices (degenerate electron or hole liquids in two-dimensional or layered nanostructures), colloidal suspensions, as well as dusty plasmas, can be mentioned [1].

The ratio of the interparticle potential energy to the kinetic energy per particle can be expressed by the *coupling parameter* defined as:

$$\Gamma = \frac{1}{4\pi\epsilon_0} \frac{Q^2}{ak_B T}, \quad (1)$$

where T is the temperature and a is the Wigner-Seitz radius. In the case of ideal plasmas $\Gamma \approx 0$, in non-ideal plasmas $\Gamma \sim 1$, while in strongly coupled plasmas $\Gamma \gg 1$. In this paper we focus on this latter, less common type of plasmas.

Strongly coupled plasmas are known to undergo crystallization at high enough density and/or low enough temperature, i.e. at high enough Γ . In the case of Coulomb systems, in three dimensions this (first order) phase transition [2] takes place at a coupling parameter value $\Gamma \cong 175$ [3, 4].

In two dimensions, for Coulomb systems the liquid phase is limited to coupling values $\Gamma \lesssim 137$, where the system is known to undergo a transition to crystallized phase [5]. Regarding Yukawa systems ($\kappa > 0$), it has been shown theoretically that exact long range order cannot exist at finite temperatures $T > 0$ [6]. Thus infinite (Yukawa) single crystals do not exist in 2D. Nonetheless, crystal-like and fluid-like behavior has been observed in 2D systems and pronounced changes of certain characteristics (e.g. bond angular order parameter) have been detected in the transition region between these two “phases” both in simulations [7] and experiments [8]. In many papers on 2D systems (most frequently 2D dusty plasma configurations) the words “phase” and “phase transition” have routinely been used. One should, however, be aware of the above mentioned arguments against the existence of true long range order and real phase transitions taking place in low dimensional Yukawa systems.

In this paper we focus on laboratory dusty plasmas, where the main constituents of the systems are micron sized dielectric particles. These particles are charged up electrically due to the electron and ion currents from the background plasma, which is provided typically by a low pressure gas discharge (see later). The interaction potential for the dust grains can be well approximated by the Yukawa type, which describes the Coulomb repulsion and the screening by the background plasma.

$$\phi(r) = \frac{Q}{4\pi\epsilon_0} \frac{\exp(-r/\lambda_D)}{r}. \quad (2)$$

Here Q is the charge of the particles and λ_D is the Debye length. The dimensionless *screening parameter* is given by:

$$\kappa = \frac{a}{\lambda_D}, \quad (3)$$

where $a = 1/\sqrt{n\pi}$ in two dimensions (n is the areal density of particles). The (nominal) plasma frequency is defined as

$$\omega_0 = \sqrt{\frac{n_{2D}Q^2}{2\epsilon_0 m a_{2D}}}. \quad (4)$$

It is noted that in 2D the plasma frequency may also have different definitions, and some of the authors use the lattice constant instead of the WS radius as a length scale.

The paper intends to give a brief account of basic features of two-dimensional and quasi-two-dimensional dusty plasmas in the strongly coupled domain [9]. The work is organized as follows. Section 2 gives a short description of the methods of our studies: the experimental realization of quasi-2D dusty plasma layers, the molecular dynamics simulation technique as well as the theoretical tool applicable for the derivation of wave dispersion relations, the Quasilocalized Charge Approximation. In section 3 representative results for the static properties (section 3.1) and collective excitations (section 3.2) are presented, and the transport properties are briefly discussed (section 3.3). A short summary is given in Section 4.

2. Methods

2.1. Experimental realization of dust plasma layers

Complex (dusty) plasmas [10, 11, 12, 13] can be created in laboratory experiments by dispersing micron-sized particles into gas discharges (see figure 1). The (typically noble gas) glow discharge can be driven either by a direct current (dc) or by a radio-frequency (rf) source, and serves primarily as a charging medium for the dielectric particles. The dust particles are exposed to electron and ion currents from the discharge plasma, and a dynamic equilibrium is rapidly reached. Their electric charge can be in the order of $\sim 10^3 - 10^4$ electron charges, depending on the diameter of the particles. The high charge of the particles gives rise to a strong electrostatic repulsion between them, and in a confined system, may lead to crystallization, see e.g. [14].

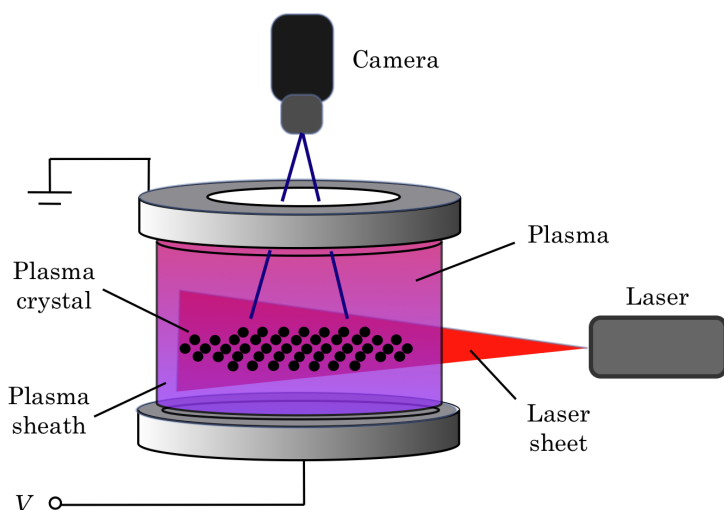


Figure 1. Experimental realization of a quasi-two-dimensional dust plasma layer.

The particles interact with their environment via several forces: gravity, ion drag force, neutral drag force, thermophoretic force, and the Lorentz force. The dominance of the different force contributions can be tuned by adjusting the experimental conditions, including choice of the particle size. In this paper we focus our attention on systems where the particles are levitated in a glow discharge with a horizontal plane-parallel electrode configuration. In this case the dominant forces are gravity and the electrostatic force arising from the “vertical” electric field of the sheath adjacent to the “lower” electrode of the discharge. These two main forces balance each other and the particles settle in a single 2D layer near the electrode sheath.

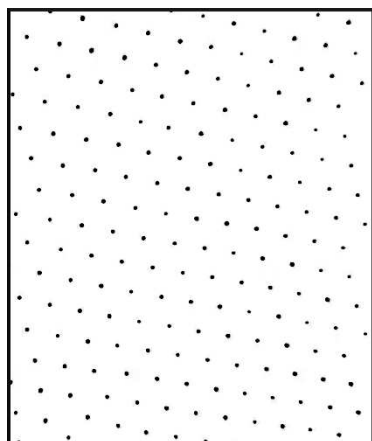


Figure 2. Snapshot (negative image) of particle configuration in a dusty plasma layer in the crystallized phase.

The number of particles which can be accommodated within a single layer is limited. If this limit is exceeded, additional layers form. The structure of these layers, especially the vertical correlations of the particle arrangements, are largely influenced by drag forces and the wake potential originating from directed ion flow. In this case particles may line up into vertical chains [15]. In this paper we restrict our studies to cases when a single layer of dust particles is formed. This layer is quasi-two-dimensional, as small displacements of the particles, perpendicular to the plane, are allowed.

The upper electrode of the discharge can be made of a mesh, or can be of solid material with a large diameter hole machined into it, this way allowing observation of the dust suspension with

a camera. The video frames can be stored by a computer, which can reconstruct the phase space trajectories of the particles. For precise determination of particle positions algorithms providing subpixel resolution have been routinely used. As an illustration a snapshot of a single-layer particle cloud is shown in figure 2. The picture was taken in an experiment using $9.16 \mu\text{m}$ diameter melamine-formaldehyde particles.

2.2. Molecular dynamics simulations

Molecular dynamics (MD) simulations follow the motion of particles by integrating their equations of motion while accounting for the pairwise interaction of the particles, as well as for the forces originating from any external field(s), see e.g. [16]. The “core” of the MD codes describes the time evolution of phase space trajectories of the ensemble of particles, while “measurements” implemented in the code provide information (from the phase space coordinates) about the quantities of interest: about density and current fluctuations, transport coefficients, as well as the pair correlation function, which gives insight into the structure of the systems and is the basis of the calculation of thermodynamic quantities.

MD simulations are applicable for both finite and infinite systems. In the case of finite systems a confinement potential keeps the system together. Infinite systems are simulated by using periodic boundary conditions; whenever a particle leaves the primary computational cell (of finite volume), it enters the same box from the opposite direction. In the simulation of quasi-two-dimensional systems periodic boundary conditions are applied in the unconfined (x and y) directions, while a confinement force acts on the particles along the z direction.

In the simulations presented here we apply the Newtonian equation of motion (in which we consider the interparticle forces and well as external confinement forces) to trace the particles in the simulation. It is noted that in dusty plasmas friction forces and randomly fluctuating forces also act on the dust particles, due to the plasma / gas background environment (see e.g. [17]). Such forces can also be considered in the simulations to improve similarity with experimental conditions, see e.g. [18, 19, 20].

In the case of Yukawa potential the forces acting on the individual particles can be calculated by summation of pairwise interaction forces, limited to a finite radius around the particles. This “cutoff” radius can be set according to the value of the screening parameter κ . In the case of small values of κ , when the cutoff radius becomes comparable with the size of the simulation box, periodic images of the computational box have to be considered in the force calculation, as well. In the limit of $\kappa \rightarrow 0$, when the Coulomb potential is recovered, periodic images up to infinity have to be included in the summation in all the principal directions. In such cases special techniques, like the Ewald summation [21, 22, 23], the fast multipole method or the particle-particle particle-mesh method (PPPM, or P3M), can be used in MD simulations [24, 25, 26, 27].

2.3. Theoretical approaches

Many body systems can be treated theoretically in a straightforward way in the extreme limits of both weak interaction and very strong interaction. In the first case, one is faced with a gaseous system, or a Vlasov plasma, where correlation effects can be treated perturbatively ($\Gamma \ll 1$). Sophisticated theoretical approaches, like diagrammatic expansions [28] make it possible to extend standard methods to obtain thermodynamic results in the moderately coupled regime. The random phase approximation (RPA) [29] method, based on the linear response theory, is a useful tool to calculate dynamical properties (wave dispersions) in the case when correlation effects are negligible.

In the case of very strong interaction, the systems crystallize, the particles are completely localized and phonons are the principal excitations. For such conditions lattice-summation techniques serve as solid basis to obtain wave dispersion information.

In the intermediate regime – in the strongly coupled liquid phase – the localization of the particles in the local minima of the potential surface still prevails, however due to the diffusion of the particles themselves the time of localization is finite [30]. A successful theoretical approach for calculating structural properties, like the $S(k)$ static structure function, is the Hyper-Netted-Chain (HNC) method, see e.g. [31].

The localization of the particles (which may typically cover a period of several plasma oscillation cycles) serves as the basis of the *Quasi-Localized Charge Approximation* (QLCA) method [32, 33], which uses structural information (in the form of $S(k)$ static structure function or $g(r)$ pair correlation function) as input for the calculations of the dispersion relations of collective modes. The conceptual basis for the QLCA has been a model that implies the following assumptions about the behavior of strongly coupled Coulomb or Yukawa liquids [32]: (i) in the potential landscape deep potential minima form that are capable of trapping (caging) charged particles; (ii) a caged charge oscillates with a frequency that is determined both by the local potential well and the interaction with the other (caged) particles in their instantaneously frozen positions; (iii) the potential landscape changes slowly to allow the charges to execute a fair number of oscillations; (iv) the escape from the cages of the particles is caused by the gradual disintegration of the caging environment; the timescale of this process is determined by the coupling strength Γ ; (v) the (time and velocity dependent) correlation between a selected pair of particles is well approximated by the (time and velocity independent) equilibrium pair correlation; (vi) the frequency spectrum calculated from the averaged (correlated) distribution of particles represents, in a good approximation the average of the distribution of frequencies originating from the actual ensemble. These assumptions have been confirmed to be reasonable in a series of studies (e.g. [30, 33]).

The main concern of the QLCA theory is the analysis of the collective behavior in strongly coupled many-particle systems. The formal tools for this are the dielectric function $\varepsilon_{\mu\nu}^{AB}(\mathbf{k}, \omega)$ [having a tensor character (subscripts) in real space and a matrix character (superscripts) in species space] and the dynamical structure function $S^{AB}(\mathbf{k}, \omega)$ or more generally, the dynamical current-current correlation function $T_{\mu\nu}^{AB}(\mathbf{k}, \omega)$. The principal approximation of the QLCA method is to replace the fluctuating microscopic densities and their products by their ensemble averages, making use of the $S(\mathbf{k})$ static structure function of the system.

All the information pertaining to the mode structure is contained in the dielectric matrix that has a longitudinal and a transverse element:

$$\varepsilon_{L/T}(\mathbf{k}, \omega) = 1 - \frac{\omega_0^2(\mathbf{k})}{\omega^2 - D_{L/T}(\mathbf{k})}. \quad (5)$$

Here the $D_L(\mathbf{k})$ and $D_T(\mathbf{k})$ local field functions are the respective projections of the QLCA dynamical matrix $D_{\mu\nu}(\mathbf{k})$ [32], which is a functional of the equilibrium pair correlation function (PCF) $h(r) \equiv g(r) - 1$ or its Fourier transform $h(\mathbf{k})$:

$$D_{\mu\nu}(\mathbf{k}) = -\frac{n}{m} \int d^2r M_{\mu\nu}(r) [e^{i\mathbf{k}\cdot\mathbf{r}} - 1] h(r) \quad (6)$$

with $M_{\mu\nu}(r) = \partial_\mu \partial_\nu \phi(r)$ being the dipole-dipole interaction potential associated with $\phi(r)$.

The dispersion relations of the longitudinal and transverse modes are determined from

$$\varepsilon_L(\mathbf{k}, \omega) = 0, \quad \varepsilon_T^{-1}(\mathbf{k}, \omega) = 0. \quad (7)$$

3. Characteristics of strongly coupled Yukawa systems

Here we present results concerning both ideal 2D Yukawa liquids [34] and quasi-2D Yukawa liquids confined (in one direction) by a parabolic potential [35]. In the latter case the particles

can freely move in the (x, y) plane, while a confinement potential $V_c(z) \propto z^2$ acts upon them when they are displaced from the $z = 0$ plane. The confinement force is linear with respect to the “vertical” displacement,

$$F_z = -f_0 \frac{Q^2}{4\pi\epsilon_0 a^3} z, \quad (8)$$

where the strength f_0 (besides Γ and κ) is the third characteristic parameter of the system. At $f_0 = 1$ the confinement force at a vertical displacement $z = a$ is equal to the magnitude of the force between two particles separated by a , interacting via Coulomb potential.

3.1. Structural properties

Figure 3 illustrates the “raw” results (particle snapshots) of MD simulations of 2D Yukawa systems at two different values of the coupling parameter Γ , belonging to the liquid phase. In the case of $\Gamma=5$ – which corresponds to a warm liquid – little correlation is seen between the particle positions, while at $\Gamma=120$ – which corresponds to a very cold liquid – the separation of the first neighbors is seen to scatter within a relatively narrow range, although no quasi-two-dimensional order is present.

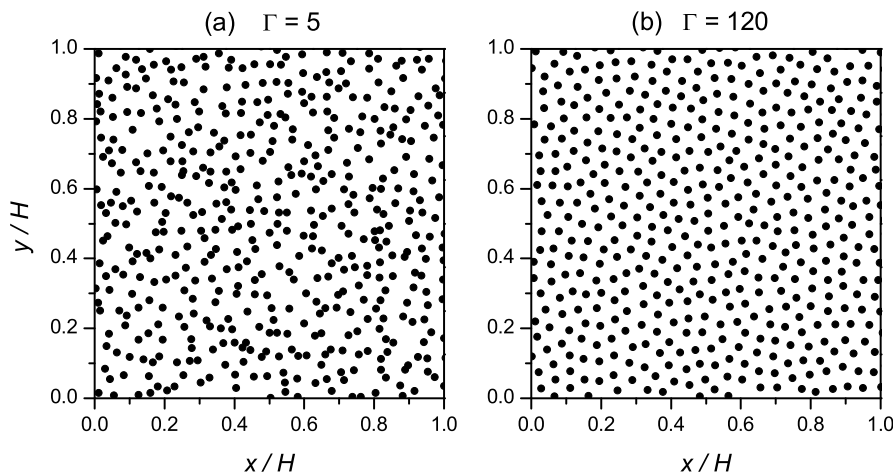


Figure 3. Snapshot of particle positions obtained in MD simulations of a 2D Yukawa liquids at (a) $\Gamma=5$ and (b) $\Gamma=120$ ($\kappa=1$). H is the edge length of the simulation box.

The degree of ordering can be quantitatively studied via the analysis of the pair correlation functions (PCFs). Figure 4 shows a series of PCFs for $\Gamma = 120$ and different κ values; all these conditions belong to the strongly coupled liquid phase. It can be seen that the pronounced order found at $\kappa = 0$ rapidly diminishes with increasing κ . (The amplitude of the first peak of the PCF can be, however, reestablished if Γ is also increased together with κ [34].) Here $\bar{r} = r/a$.

In the case of parabolic confinement the number of layers formed in the system depends on the strength of the confinement. Figure 5(a) shows the distribution of particle density along the z direction, $n(z)$, for different strengths of confinement (f_0), at $\Gamma = 100$ and $\kappa = 0.27$ (belonging to the liquid phase). We observe a transition from two-layered configuration to a single layer at $f_0 \approx 1.4$. Due to the finite temperature of the system the layers do not resemble crystal planes (like in ion trap experiments) but they are rather broad. At $f_0 = 1.4$ the width of the layer is $\approx 0.86a$ (at half of the maximum of the distribution). Doubling the amplitude of the potential results in a width $0.17a$. When the repulsion between the particles decreases at higher κ values, the potential with the same amplitude results in a stronger confinement. Thus, with increasing

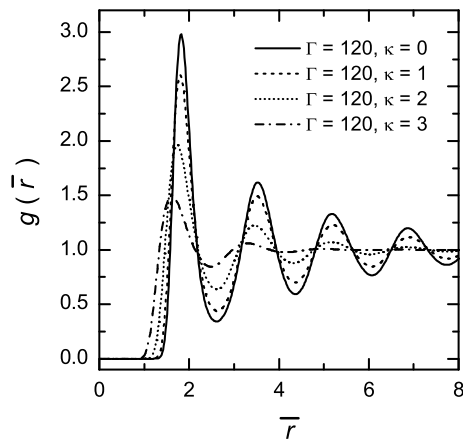


Figure 4. Pair correlation functions of 2D Yukawa liquids at $\Gamma = 120$, for different values of the screening parameter. Reproduced from Ref. [34]; copyright (2005) by the American Physical Society.

κ the number of layers, or the width of the single layer decreases, as illustrated in Fig. 5(b). Similar studies of layer formation in quasi-2D systems have been presented in [36, 37, 38].

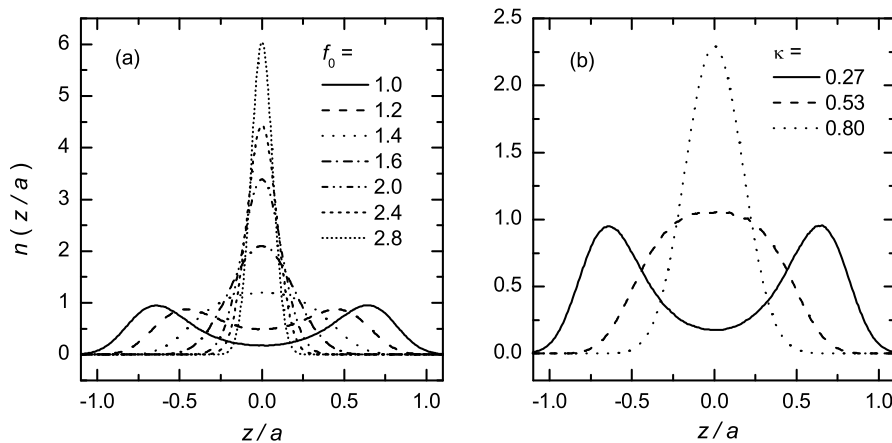


Figure 5. Density distribution of particles along the z direction in the quasi-2D system (normalized as $\int n(z/a)d(z/a) = 1$). (a) Dependence on the strength of confinement at $\Gamma = 100$ and $\kappa = 0.27$; (b) Dependence on κ at constant f_0 . Reproduced from Ref. [35]; copyright (2004) by the American Physical Society.

Our further studies of the collective excitations (to be presented in the forthcoming section) concern the domain of parameters when a *single layer* is formed. At higher number of layers the mode structure is expected to be more complicated [39] but this is not within the scope of the present paper.

3.2. Collective excitations

The different waves that can build up in a quasi-two-dimensional dust plasma layer are shown in figure 6. In an ideally narrow layer only the compressional (\mathcal{L}) and in-plane transverse modes (\mathcal{T}) exist, while in the case of a layer of finite width (confined e.g. by a parabolic potential) a third collective mode, the out-of-plane transverse mode (\mathcal{P}) can also develop.

In the MD simulation information about the (thermally excited) collective modes and their dispersion is obtained from the Fourier analysis of the correlation spectra of the density and

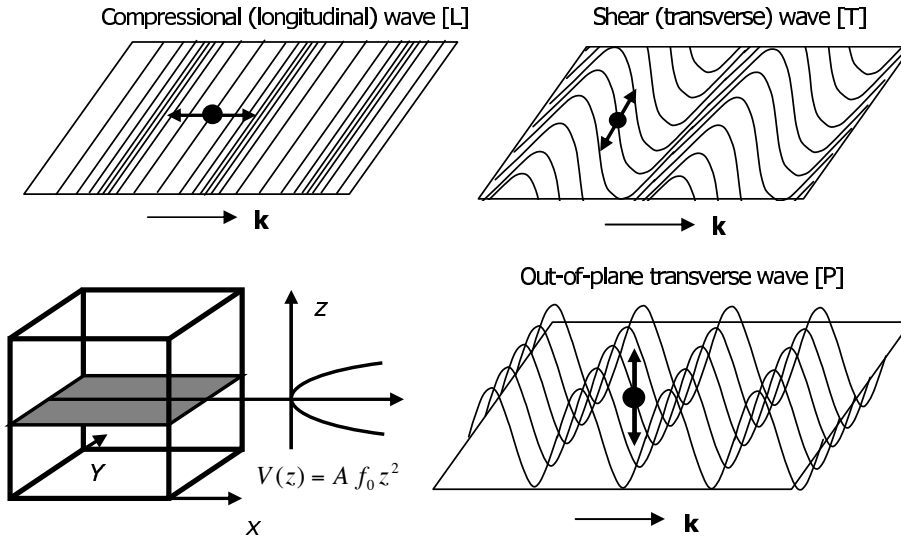


Figure 6. Types of collective excitations in a quasi-two-dimensional dust plasma layer.

current fluctuations. Taking as an example the microscopic density defined as

$$\rho(k, t) = \sum_j \exp[ikx_j(t)], \quad (9)$$

the dynamical structure function is obtained by the following expression [40]:

$$S(k, \omega) = \frac{1}{2\pi N} \lim_{\Delta T \rightarrow \infty} \frac{1}{\Delta T} |\rho(k, \omega)|^2, \quad (10)$$

where $\rho(k, \omega) = \mathcal{F}[\rho(k, t)]$ is the Fourier transform of (9). Similarly, the spectra of the longitudinal and transverse current fluctuations, $L(k, \omega)$, as well as $T(k, \omega)$ and $P(k, \omega)$, respectively, can be obtained from Fourier analysis of the quantities

$$\begin{aligned} \lambda(k, t) &= k \sum_j v_{jx}(t) \exp[ikx_j(t)], \\ \tau(k, t) &= k \sum_j v_{jy}(t) \exp[ikx_j(t)], \\ \pi(k, t) &= k \sum_j v_{jz}(t) \exp[ikx_j(t)], \end{aligned} \quad (11)$$

where x_j and v_j are the position and velocity of the j -th particle. Here we assume that \mathbf{k} is directed along the x axis (the system is isotropic) and accordingly omit the vector notation of the wave number. The spectra are obtained for a series of wave numbers, which are multiples of $k_{\min} = 2\pi/H$, where H is the edge length of the simulation box. The dimensionless wave number is defined as: $\bar{k} = ka$.

Figure 7 shows the energy density of the different type current-current fluctuations on the $\omega - k$ plane.

The dispersion relations of the quasi-2D Yukawa system are displayed in Figure 8 for different values of f_0 and κ . $\Gamma = 100$ for all the cases, and thus the systems are in the liquid phase, where

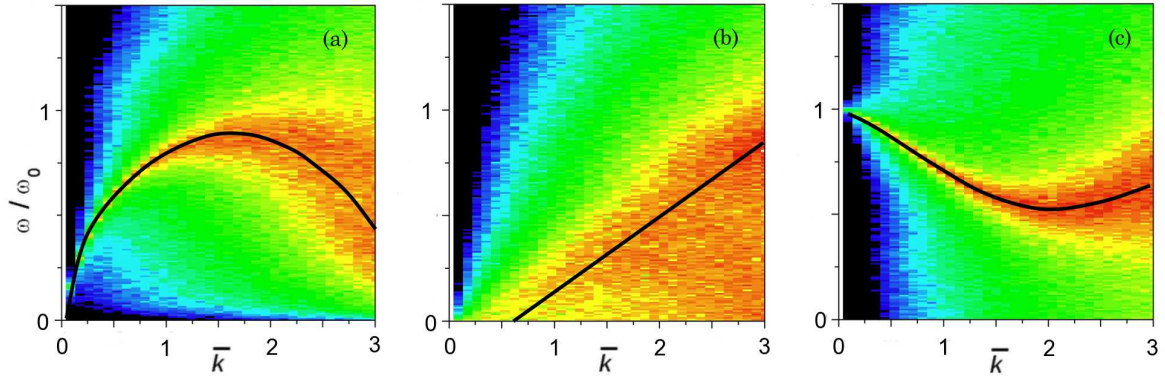


Figure 7. (Color online) Spectral composition of the energy of thermally excited waves in a quasi-2D dusty plasma system in the liquid phase at $\Gamma = 100$, $\kappa = 0.27$, and $f_0 = 2$. (a) Longitudinal, (b) in-plane transverse, and (c) out-of-plane transverse modes. The color scales are logarithmic, they intend to illustrate qualitative features only. Red color indicates concentration of the energy, the heavy black lines are approximate dispersion relations.

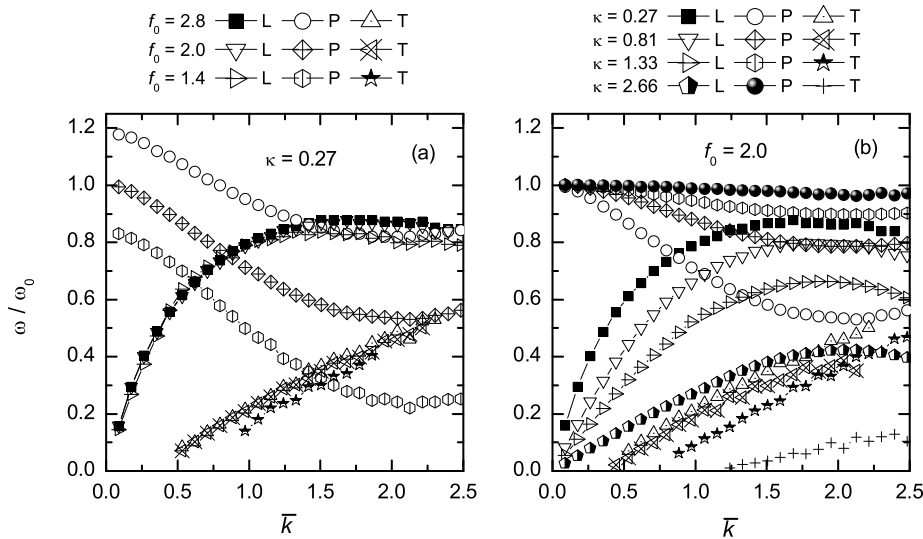


Figure 8. Dispersion relations of quasi-2D Yukawa liquids for (a) $\kappa = 0.27$ and different values of the amplitude f_0 of the confining potential, and (b) for fixed $f_0 = 2$ and different values of the screening parameter κ . Reproduced from Ref. [35]; copyright (2004) by the American Physical Society.

all directions are equivalent and the dispersion relations are isotropic. At constant κ , as shown in Figure 8(a), the frequency of the out-of-plane transverse mode changes significantly as the strength of the confinement force, f_0 , is varied. At $k = 0$ the whole layer oscillates in unison in the potential well with a frequency $\omega(k = 0) = \sqrt{f_0 c/m}$, which gives $\frac{\omega(k=0)}{\omega_0} = \sqrt{f_0/2}$. A decreasing confinement force amplitude results in a smaller $\omega(k = 0)$ and $\omega(k \rightarrow \infty)$.

The \mathcal{L} and \mathcal{T} modes are only slightly affected by the value of f_0 . The frequency of these modes is somewhat smaller at $f_0 = 1.4$, which is near the lower bound of f_0 for the formation of a single layer [35]. The \mathcal{L} mode exhibits a quasi acoustic behavior, while the \mathcal{T} mode shows

an acoustic, $\omega \propto k$ dispersion, with a cutoff at a finite wave number. For the \mathcal{P} mode we find $d\omega/dk < 0$ in the $\bar{k} \lesssim 2.1$ domain. Beyond this wave number the frequency of the mode slightly increases. This observation on the liquid system agrees well with that on the crystallized system [41], where the same behavior was found, except that in the latter system the critical wave number (at which the group velocity $d\omega/dk$ changes from negative to positive) also depends on the direction of the propagation in the lattice. At a constant f_0 the value of $\omega(k=0)$ does not change when κ is varied, but – as shown in Figure 8(b) – $\omega(k > 0)$ increases with increasing κ . This is explained by the decreased interparticle force (at an average particle separation) at higher κ .

The dispersion relations of 2D Yukawa liquids generated by MD simulations have been cross checked with theoretical (QLCA) results in [42]. Dispersion characteristics can also be derived from experimental studies by tracking the phase space trajectories of the particles, which allows the calculation of the fluctuation spectra just like in the case of the simulations. Such studies have been presented e.g. in [43] and [44] for the solid phase and in [45] for the liquid phase of Yukawa systems.

3.3. Transport properties

MD methods offer two basic ways to study transport processes. In *non-equilibrium* MD simulation methods an external perturbation is applied to the system and the system's response (linked to the perturbation through a transport coefficient) is measured. In *equilibrium* simulations time correlation functions of certain microscopic quantities are measured and the macroscopic transport coefficients are obtained through the Green-Kubo (GK) relations. For the self-diffusion (D_s), shear viscosity (η), and thermal conductivity (λ) the GK relations are given as [46]:

$$D_s = \frac{1}{\mathcal{D}} \int_0^\infty C_v dt, \quad C_v \equiv \langle \mathbf{v}(t) \cdot \mathbf{v}(0) \rangle, \quad (12)$$

$$\eta = \frac{1}{VkT} \int_0^\infty C_\eta dt, \quad C_\eta \equiv \langle P_{ij}(t)P_{ij}(0) \rangle, \quad (13)$$

$$\lambda = \frac{1}{VkT^2} \int_0^\infty C_\lambda dt, \quad C_\lambda \equiv \langle J_{Qi}(t)J_{Qi}(0) \rangle. \quad (14)$$

In the above formulae C_v , C_η , and C_λ are the velocity (VACF), shear stress (SACF) and energy current (EACF) autocorrelation functions, respectively. The calculation of these correlation functions requires time series for the particle velocity \mathbf{v} , the off-diagonal element of the pressure tensor P_{ij} , and the energy current J_{Qi} . Here, \mathcal{D} is the dimensionality of the system and $i \neq j$ are space coordinates.

For the existence of transport coefficients the integrands in Eqs. (12)-(14) must converge. This may not always be the case in some lower dimensional ($\mathcal{D} < 3$) systems. Non-exponential long-time tails in the VACF of hard sphere and hard disk systems were first reported by Alder and Wainwright [47] based on their simulation studies. They have found a $t^{-\mathcal{D}/2}$ decay in these systems. According to this finding, for $\mathcal{D}=2$ the VACF is non-integrable, and consequently the diffusion coefficient does not exist. Further, it has been shown [48] that the kinetic contributions to the autocorrelation functions of shear stress and energy current – which are related to velocity correlations – exhibit the same behavior. Their findings were also confirmed by the calculations in [49]. Regarding systems with continuous potentials, a power law decay of the VACF was observed in 3D soft-repulsive and Lennard-Jones liquids [50], as well as a t^{-1} tail of the SACF was detected in the molecular dynamics simulations of a 2D soft disk fluid [51]. For the case of Coulomb interaction (2D classical electron liquid) the existence of self-diffusion coefficient has been a topic of controversy [52, 53, 54].

While the $t^{-3/2}$ decay in case of $\mathcal{D} = 3$ allows for an integrable VACF and thus for a meaningful diffusion coefficient to exist, in two dimensions, the corresponding $t^{-\mathcal{D}/2} = t^{-1}$ decay makes the VACF non-integrable. Thus the analysis of transport properties in 2D systems is of great interest and has already been the topic of some recent papers. As an example the equilibrium MD simulations of 2D Yukawa liquids by Liu and Goree [55] may be mentioned. In this study it was demonstrated that *superdiffusion* rather than normal diffusion occurs over a wide range of temperatures (at $\kappa = 0.56$).

The emergence and vanishing of superdiffusion in quasi-two-dimensional Yukawa systems (“bridging the gap” between 2D and 3D systems) have been investigated by molecular dynamics simulations by Ott *et al.* [56]. In this work the systems have been confined by two different potentials: (i) a parabolic potential and (ii) a soft box potential. Both of these potentials allowed a smooth change of the character of the system between a three-dimensional one and a two-dimensional one. The existence of a transition from normal diffusion to superdiffusion was identified in [56] by analyzing both the asymptotic behavior of the mean-squared displacement of the particles and the long-time tail of the velocity autocorrelation function.

Self-diffusion has also been experimentally studied in a two-dimensional underdamped laboratory liquid complex (dusty) plasmas by Nunomura *et al.* [57]. No superdiffusion has been observed in this work, but subdiffusion occurred at temperatures close to melting. Anomalous diffusion and non-Gaussian statistics have, on the other hand, been detected experimentally in a two-dimensional driven-dissipative Yukawa system by Liu and Goree [58]. In their experiment a single-layer dusty plasma suspension with a Yukawa interaction and frictional dissipation has been heated with laser radiation pressure to yield a structure with liquid ordering. Analyzing the time series for mean-square displacement, superdiffusion has been detected at a low but statistically significant level over a wide range of temperatures. Mass transfer processes have recently thoroughly been analyzed by Vaulina and coworkers both experimentally [59] and through numerical simulation [18].

Clarification of the behavior of the shear stress and energy current autocorrelation functions (SACF and EACF) of 2D Yukawa systems is a topic of current work [60]. The analysis of the long-time behavior of these functions is considerably more difficult as compared to the VACF, since, while the calculation of the VACF includes an averaging over a high number of particles and different initial times, for the SACF and EACF only the latter averaging is involved. Consequently the signal to noise ratio of the data obtained in a single simulation run for the SACF and the VACF may be orders of magnitude inferior compared to that of the VACF, and reaching of acceptable signal to noise levels requires numerous simulation runs with different initial conditions. Nonetheless, with the advance of computational resources details of the long-time behavior of the SACF and EACF of 2D and quasi-2D Yukawa liquids are also expected to be uncovered.

4. Summary

This paper intended to review some prominent features of strongly coupled 2D and quasi-2D Yukawa systems. The combination of theoretical and simulation methods on one hand, and the possibility of experimental realization of such many-particle systems, on the other hand, provides their fairly complete characterization.

We have presented here static properties, illustrated collective effects and briefly reviewed transport characteristics of such systems. While the first two of these are fairly well understood, further work is needed to shed light on the transport properties in the low-dimensional systems considered here.

5. Acknowledgment

This work has been supported by the Hungarian Fund for Scientific Research (OTKA-T-048389, OTKA-IN-69892, OTKA-PD-75113), by a bilateral grant between the Hungarian Academy of Sciences and the National Science Foundation of USA (MTA/NFS-102), by the National Science Foundation (PHY-0514619) and by the Janos Bolyai Research Scholarship of the Hungarian Academy of Sciences (PH).

References

- [1] Kalman G J, Rommel J M and Blagoev K 1998 *Strongly Coupled Coulomb Systems (New York: Plenum)*; Special Issue 2003 *J. Phys. A: Math. Gen.* **36** no. 22; Special Issue 2006 *J. Phys. A: Math. Gen.* **39** no. 17.
- [2] Brush S G, Sahlin H L and Teller E L 1966 *J. Chem. Phys.* **45** 2102
- [3] Stringfellow G S, DeWitt H E and Slattery W L 1990 *Phys. Rev. A* **41** 1105
- [4] Farouki R T and Hamaguchi S 1993 *Phys. Rev. E* **47** 4330
- [5] Grimes C C and Adams G 1976 *Phys. Rev. Lett.* **36** 145
- [6] Peierls R E 1935 *Ann. Inst. Henri Poincaré* **5** 177; Landau L D 1937 *Phys. Z. Sovjet.* **11** 26; Hohenberg P C 1966 *Phys. Rev.* **158** 383; Mermin N D 1968 *Phys. Rev.* **176** 250
- [7] Totsuji 2001 *Physics of Plasmas* **8** 1856 Hartmann P, Donkó Z, Bakshi P, Kalman G J and Kyrkos S 2007 *IEEE Trans. Plasma Sci.* **35** 332
- [8] Melzer A, Homann A and Piel A 1996 *Phys. Rev. E* **53** 2757; Quinn R A and Goree J 2001 *Phys. Rev. E* **64** 051404
- [9] Donkó Z, Kalman G J and Hartmann P 2008 *J. Phys. Cond. Matter* **20** 413101
- [10] Mendis D A 2002 *Plasma Sources Sci. Technol* **11** A219
- [11] Merlino R L and Goree J A 2004 *Physics Today* **57** 32
- [12] Fortov V E, Ivlev A V, Khrapak S A, Khrapak A G and Morfill G E 2005 *Phys. Rep.* **421** 1
- [13] Ishihara O 2007 *J. Phys. D: Appl. Phys.* **40** R121
- [14] Thomas H, Morfill G E, Demmel V, Goree J, Feuerbacher B and Möhlmann D 1994 *Phys. Rev. Lett.* **73** 652
Chu J H and Lin I 1994 *Phys. Rev. Lett.* **72** 4009; Hayashi Y, Tachibana K 1994 *Japan. J. Appl. Phys.* **33** L814
Melzer A, Trottenberg T and Piel A 1994 *Phys. Lett. A* **191** 301
- [15] Lampe M, Joyce G, Ganguli V Gavrishchaka V 2000 *Phys. Plasmas* **7** 3851; Hebner G A and Riley M E 2004 *Phys. Rev. E* **69** 026405
- [16] Frenkel D and Smit B 2001 *Understanding Molecular Dynamics Simulations* (Academic Press).
- [17] Baimbetov F B, Ramazanov T S, Dzhumagulova K N, Kadysizov E R, Petrov O F and Gavrikov A V 2006 *J. Phys. A: Math. Gen.* **39** 4521
- [18] Vaulina O S, Adamovich X G, Petrov O F and Fortov V E 2008 *Phys. Rev. E* **77** 066403
- [19] Feng Y, Liu Bin and Goree J 2008 *Phys. Rev. E* **78** 026415
- [20] Hou L-J and Piel A 2008 arXiv:0810.1623v1 [physics.plasm-ph]
- [21] Ewald P P 1921 *Ann. Phys.* **64** 253
- [22] Salin G and Caillol J-M 2002 *Phys. Rev. Lett.* **88** 065002; 2003 *Phys. Plasmas* **10** 1220.
- [23] Johnson R E and Ranganathan S 2001 *Phys. Rev. E* **63** 056703
- [24] Sagui C and Darden T A 1999 *Ann. Rev. Biophys. Biomol. Struct.* **28** 155
- [25] David N and Hooker S M 2003 *Phys. Rev. E* **68** 056401
- [26] David N, Spence D J and Hooker S M 2004 *Phys. Rev. E* **70** 056411
- [27] Eastwood J W, Hockney R W and Lawrence D N 1980 *Comput. Phys. Commun.* **19** 215; Hockney R and Eastwood J 1981 *Computer Simulation Using Particles* (New York: McGraw-Hill)
- [28] Hansen J P, McDonald I R 1976 *Theory of Simple Liquids* (Academic Press, London)
- [29] Ehrenreich H and Cohen M H 1959 *Phys. Rev.* **115** 786
- [30] Donkó Z, Kalman G J and Golden K I 2002 *Phys. Rev. Lett.* **88** 225001
- [31] Lado F 1978 *Phys. Rev. B* **17** 2827; Rogers F J, Young D A, DeWitt H E and Ross M 1983 *Phys. Rev. A* **28** 2990
- [32] Golden K I and Kalman G J 2000 *Phys. Plasmas* **7** 14
- [33] Kalman G J, Golden K I, Donkó Z and Hartmann P 2005 *J. Phys. Conf.* **11** 254
- [34] Hartmann P, Kalman G J, Donkó Z and Kutasi K 2005 *Phys. Rev. E* **72** 026409
- [35] Donkó Z, Hartmann P and Kalman G J 2004 *Phys. Rev. E* **69** 065401
- [36] Totsuji H, Kishimoto T, Inoue Y, Totsuji C and Nara S 1996 *Phys. Lett. A* **221** 215
- [37] Bystrenko O 2003 *Phys. Rev. E* **67** 025401
- [38] Qiao K and Hyde T W 2005 *Phys. Rev. E* **71** 026406

- [39] Donkó Z, Kalman G J, Hartmann P, Golden K I and Kutasi K 2003 *Phys. Rev. Lett.* **90** 226804; Donkó Z, Hartmann P, Kalman G J and Golden K I 2003 *J. Phys. A: Math. Gen.* **36** 5877
- [40] Hansen J P, McDonald I R and Pollock E L 1975 *Phys. Rev. A* **11** 1025
- [41] Qiao K and Hyde T W 2003 *Phys. Rev. E* **68** 046403
- [42] Kalman G J, Hartmann P, Donkó Z, Rosenberg M 2004 *Phys. Rev. Lett.* **92** 065001
- [43] Nunomura S, Goree J, Hu S, Wang X and Bhattacharjee A 2002 *Phys. Rev. E* **65** 066402
- [44] Nunomura S, Goree J, Hu S, Wang X, Bhattacharjee A and Avinash K 2002 *Phys. Rev. Lett.* **89** 035001
- [45] Nunomura S, Zhdanov S, Samsonov D and Morfill G E 2005 *Phys. Rev. Lett.* **94** 045001
- [46] Hansen J-P and McDonald I R 1976 *Theory of simple liquids* (Academic Press, New York)
- [47] Alder B J and Wainwright T E 1970 *Phys. Rev. A* **1** 18
- [48] Ernst M H, Hauge E H and van Leeuwen J M J 1970 *Phys. Rev. Lett.* **25** 1254
- [49] Dorfman J R and Cohen E G D 1972 *Phys. Rev. A* **6** 776
- [50] McDonough A, Russo S P and Snook I K 2001 *Phys. Rev. E* **63** 026109
- [51] Morriss G P and Evans D J 1985 *Phys. Rev. A* **32** 2425
- [52] Hansen J P, Levesque D and Weis J J 1979 *Phys. Rev. Lett.* **43** 979
- [53] Baus M and Bosse J 1980 *Phys. Rev. A* **22** 2284
- [54] Agarwal G K and Pathak K N 1983 *J. Phys. C: Solid State Phys.* **16** 1887
- [55] Liu Bin and Goree J 2007 *Phys. Rev. E* **75** 016405
- [56] Ott T, Donkó Z, Hartmann P and Bonitz M 2008 *Phys. Rev. E* **78** 026409
- [57] Nunomura S, Samsonov D, Zhdanov S and Morfill G 2006 *Phys. Rev. Lett.* **96** 015003
- [58] Liu Bin and Goree J 2008 *Phys. Rev. Lett.* **100** 055003
- [59] Vaulina O S, Adamovich X G, Petrov O F and Fortov V E 2008 *Phys. Rev. E* **77** 066404
- [60] Donkó Z, Goree J, Hartmann P and Liu Bin 2008 in preparation